

1 Assimilation of sediments embedded in the oceanic arc
2 crust: myth or reality?

3 Rachel Bezard^{1,2*}, Jon P. Davidson¹, Simon Turner², Colin G. Macpherson¹, Jan M.
4 Lindsay³ and Adrian J. Boyce⁴

5 ¹ *Northern Centre for Isotopic and Elemental Tracing (NCIET), Department of Earth
6 Sciences, Durham University, South Road, Durham DH1 3LE, UK*

7 ² *CCFS/GEMOC, Department of Earth and Planetary Sciences, Macquarie University,
8 University Avenue, Macquarie Park NSW 2113, Australia*

9 ³ *School of Environment, The University of Auckland, Private Bag 92019, Auckland
10 1142, New Zealand*

11 ⁴ *Scottish Universities Environment Research Center, Rankine Avenue East Kilbride
12 Glasgow G75 0QF, Scotland*

13 *Corresponding Author. Tel.: +61298504406; Fax: +61298508943; E-mail address: rachel.bezard@students.mq.edu.au

14 ABSTRACT

15 Arc magmas are commonly assumed to form by melting of sub-arc mantle that has been
16 variably enriched by a component from the subducted slab. Although most magmas that
17 reach the surface are not primitive, the impact of assimilation of the arc crust is often
18 ignored with the consequence that trace element and isotopic compositions are commonly
19 attributed only to varying contributions from different components present in the mantle.
20 This jeopardises the integrity of mass balance recycling calculations. Here we use Sr and
21 O isotope data in minerals from a suite of volcanic rocks from St Lucia, Lesser Antilles
22 arc, to show that assimilation of oceanic arc basement can be significant. Analysis of
23 $^{87}\text{Sr}/^{86}\text{Sr}$ in single plagioclase phenocrysts from four Soufrière Volcanic Complex (SVC;
24 St Lucia) hand samples with similar composition ($^{87}\text{Sr}/^{86}\text{Sr} = 0.7089\text{-}0.7091$) reveals
25 crystal isotopic heterogeneity among hand samples ranging from 0.7083 to 0.7094 with up
26 to 0.0008 difference within a single hand sample. $\delta^{18}\text{O}$ measurements in the SVC crystals
27 show extreme variation beyond the mantle range with +7.5 to +11.1‰ for plagioclase
28 (n=19), +10.6 to +11.8‰ for quartz (n=10), +9.4 to +9.8‰ for amphibole (n=2) and +9
29 to +9.5‰ for pyroxene (n=3) while older lavas (Pre-Soufrière Volcanic complex), with less
30 radiogenic whole rock Sr composition ($^{87}\text{Sr}/^{86}\text{Sr} = 0.7041\text{-}0.7062$) display values closer to
31 mantle range: +6.4 to +7.9‰ for plagioclase (n=4) and +6 to +6.8‰ for pyroxene (n=5).
32 We argue that the $^{87}\text{Sr}/^{86}\text{Sr}$ isotope disequilibrium and extreme $\delta^{18}\text{O}$ values provide
33 compelling evidence for assimilation of material located within the arc crust. Positive
34 correlations between mineral $\delta^{18}\text{O}$ and whole rock $^{87}\text{Sr}/^{86}\text{Sr}$, $^{143}\text{Nd}/^{144}\text{Nd}$ and
35 $^{206,207,208}\text{Pb}/^{204}\text{Pb}$ shows that assimilation seems to be responsible not only for the isotopic
36 heterogeneity observed in St Lucia but also in the whole Lesser Antilles since St Lucia

37 encompasses almost the whole-arc range of isotopic compositions. This highlights the need
38 for detailed mineral-scale investigation of oceanic arc suites to quantify assimilation that
39 could otherwise lead to misinterpretation of source composition and subduction processes.

40 **1.Introduction**

41 A key question in oceanic arc geochemistry concerns the relative contributions of
42 subducting slab and intra-crustal material in the chemical and isotopic characteristics of
43 lavas. Oceanic arc magmas are generated by partial melting of the mantle wedge modified
44 by H₂O-rich fluids and melts from the subducting slab (Tatsumi and Eggins, 1995) and
45 subsequently ascend through the arc crust before eruption. Lavas erupted at oceanic arcs
46 rarely have major element compositions in equilibrium with mantle peridotite (Annen et
47 al, 2006) which suggests that the magmas experienced differentiation during storage within
48 or at the base of the arc crust. Depending on the nature of the arc basement, such magmas
49 may interact with igneous or metasedimentary wall rocks during differentiation.
50 Distinguishing between sediment addition to the mantle wedge and assimilation of
51 metasediments located in the arc crust is not straightforward on the basis of whole rock
52 compositions alone– the effects of mixing sediment into the mantle wedge or with basaltic
53 melts in the crust are similar in most radiogenic isotope-isotope spaces.

54 In order to investigate the role of crustal assimilation in oceanic arcs we selected a suite of
55 rocks from the Lesser Antilles arc where, despite the absence of continental basement,
56 whole rock isotope ratios of arc lavas can be very “continental”. As a result, the case has
57 long been made both for crustal assimilation (e.g. Davidson, 1987; Davidson and Harmon,
58 1989; Smith et al., 1996; Thirlwall et al., 1996; Thirlwall and Graham, 1984; Van Soest et
59 al., 2002), and incorporation of sediment or sediment melt into the mantle wedge (e.g.
60 Carpentier et al., 2008; 2009; Labanieh et al., 2010; 2012; White and Dupré, 1986). Our
61 suite of samples, from the island of St Lucia, encompasses almost the entire range of whole
62 rock isotopic compositions observed in the Lesser Antilles, ranging from values close to

63 typical intra-oceanic arc rocks to those resembling continental crust (e.g. $^{87}\text{Sr}/^{86}\text{Sr}$,
64 $^{143}\text{Nd}/^{144}\text{Nd}$ and $^{206}\text{Pb}/^{204}\text{Pb}$ ranging from 0.70411-0.70906, 0.51210-0.51298 and 19.291-
65 19.797 respectively). $^{87}\text{Sr}/^{86}\text{Sr}$ and $\delta^{18}\text{O}$ analyses of individual minerals separated from
66 lavas with extreme crust-like whole rock isotopic composition from the Soufriere Volcanic
67 Complex (SVC), demonstrate the importance of open system behaviour on oceanic arc
68 magmatism and challenge our understanding of magma differentiation in oceanic arcs.

69 **2.Geological background**

70 The Lesser Antilles arc (Fig. 1) formed as a result of subduction of the North American
71 Plate under the Caribbean Plate. Its lavas have typical oceanic arc compositions in the
72 northern section but unusually heterogeneous isotopic signatures in the central and
73 southern part of the arc where both typical intra-oceanic arc and very continental crust-like
74 signatures are observed (e.g. Macdonald et al., 2000; Fig.2). Two main processes have been
75 proposed to explain these extreme compositions: (1) incorporation of sediment into the
76 mantle source or (2) significant assimilation of sediment-rich arc crust. While a high
77 sediment input to the source could be explained by the presence of abundant sediment in
78 the southern Antilles Trench, due to discharge from the Orinoco and Amazon rivers (e.g.
79 Carpentier et al., 2008; 2009), assimilation of sediment in the arc crust is also possible
80 because the central-southern Lesser Antilles arc is thought to have developed above the
81 thick forearc basin of the (now extinct) Aves Ridge Arc, splitting it into the Grenada and
82 the Tobago basins (Fig. 1; Aitken et al., 2011). Sediments entering the subduction zone are
83 chemically and isotopically well constrained by analyses from DSDP Sites 144 and 543
84 (Fig.1; Carpentier et al., 2008; 2009; White and Dupré, 1986). In contrast, the nature of the
85 basement of the Southern Lesser Antilles arc is still poorly known. While the detrital

86 sediments from the South American craton, which dominate the sequences on both the
87 subducting and the overriding plates, were often targeted in the past to explain the high
88 $^{87}\text{Sr}/^{86}\text{Sr}$ and low $^{143}\text{Nd}/^{144}\text{Nd}$ ratios of the lavas, they fail to explain their very radiogenic
89 Pb signatures. Recently, analyses of Mesozoic black shales sampled at DSDP site 144
90 showed that these sediments have sufficiently radiogenic Pb to account for the
91 compositions of the lavas from the southern arc (Carpentier et al., 2009). Because such
92 radiogenic Pb has not yet been reported from the sediments of the Grenada and Tobago
93 basins, sediment addition to the source alone has been suggested to explain the whole range
94 of isotopic data in the southern arc lavas (Carpentier et al., 2008; 2009; Labanieh et al.,
95 2010). However, it cannot be ruled out that such sediments exist within the basement of
96 the southern arc since biogenic rich limestones have been reported in the overriding plate,
97 in the Late Cretaceous to Oligocene sequences of the Carupano Basin (Ysaccis, 1997).

98

99 St Lucia is an island in the central-southern part of the arc (Fig.1). The lavas from this
100 single island encompass almost the whole range of isotopic variation observed in the arc
101 making it the perfect location to study the influence of crustal components (Fig.2). The
102 more continental crust-like compositions are found in andesites (3Ma to ca. 250 ka) and
103 dacites (100 ka to present) of the Soufriere Volcanic Complex (SVC), while more mantle-
104 like compositions are observed in the more mafic Pre-SVC lavas dominated by basalt,
105 basaltic andesite and andesite (18 Ma to 1.1 Ma; Briden et al., 1979; De Kerneison et al.,
106 1983; Lindsay et al., 2013; Samper et al., 2008; Schmidt et al., 2010).

107 **3.Methods**

108 *3.1. Whole rock Sr, Nd and Pb isotopes*

109 Except for 7 samples in which Sr and Nd isotope ratios were measured at the Geochemical
110 Analysis Unit at Macquarie University (Aus), whole rock powders were analysed at the
111 Arthur Holmes Isotope Geology Laboratory (AHIGL) which is part of Durham
112 Geochemistry Centre (DGC) at Durham University (UK) At both institutes, 0.1 g of sample
113 powder was dissolved in Teflon distilled 29M HF and 16M HNO₃.

114 At Durham, Pb and Sr were separated from the sample solution using Sr-spec resin
115 columns. Nd was collected from the same Sr-spec column before being passed through a
116 cation column where it was collected as part of a total REE cut after elution of Hf, Rb and
117 Ba. Samples were analysed for their ⁸⁷Sr/⁸⁶Sr, ¹⁴³Nd/¹⁴⁴Nd and ²⁰⁶Pb/²⁰⁴Pb, ²⁰⁷Pb/²⁰⁴Pb and
118 ²⁰⁸Pb/²⁰⁴Pb compositions by plasma ionisation multicollector mass spectrometry (PIMMS)
119 using a Thermo Scientific Neptune instrument. During the ⁸⁷Sr/⁸⁶Sr and ¹⁴³Nd/¹⁴⁴Nd
120 analytical sessions, instrument performance was monitored by analysis of NBS987 Sr
121 standard and an in house J&M Nd standards and within-run instrument mass fractionation
122 was corrected using an exponential law and the normalising value of ⁸⁸Sr/⁸⁶Sr = 8.375209
123 and ¹⁴⁶Nd/¹⁴⁵Nd = 2.079143 respectively (equivalent to ⁸⁶Sr/⁸⁸Sr = 0.1194 and ¹⁴⁶Nd/¹⁴⁴Nd
124 = 0.7219). Since Nd was analysed as part of a total REE cut, the data requires an algebraic
125 correction for Sm interference on Nd based on the approach of Nowell and Parrish (2001).
126 The accuracy of this correction was monitored by analysis of Sm-doped J&M, with a
127 Sm/Nd ratio of ~0.25. The average ⁸⁷Sr/⁸⁶Sr for NBS987 was 0.710272 ± 0.000020 (2sd;
128 n=14) and the average ¹⁴³Nd/¹⁴⁴Nd for both pure and Sm-doped J&M was 0.511105 ±
129 0.00002 (2sd; n=15). ⁸⁷Sr/⁸⁶Sr ratios are reported relative to NBS987 standard value of
130 0.71024 (Thirlwall, 1991) and ¹⁴³Nd/¹⁴⁴Nd is reported relative to a J&M standard value of
131 0.511110 which is equivalent to a La Jolla value of 0.511862 (Royse et al., 1998). The

132 $^{87}\text{Sr}/^{86}\text{Sr}$ and $^{143}\text{Nd}/^{144}\text{Nd}$ ratios of the two international rock standards BHVO-1 and BIR-
133 1 were 0.703463 and 0.512989 and 0.703115 and 0.513073 respectively. The accuracy of
134 the Sm correction on the $^{143}\text{Nd}/^{144}\text{Nd}$ ratio is illustrated by the analysis of BHVO-1, which
135 after Sm correction is identical to the ratio of 0.512986 ± 0.000009 (2sd; n=19) that Weiss
136 et al. (2005) obtained by thermal ionisation mass spectrometry (TIMS).

137 Following chemistry, the Pb fractions were taken up in 1 ml of 3% HNO_3 . The Pb
138 concentration of the aliquots was analysed before isotopic measurements, in order to
139 calculate the appropriate amount of Tl spike to add to obtain a Pb/Tl ratio of ~ 12 . This
140 minimizes the tail from ^{205}Tl onto ^{204}Pb and from ^{206}Pb onto ^{204}Tl . During isotopic
141 measurements, the samples were introduced into the Neptune using an ESI PFA50
142 nebulizer and a cyclonic spray-chamber. The normal H skimmer cone was used. Sensitivity
143 for Pb on the Neptune using such setup is typically around 100 V total Pb ppm^{-1} at an
144 uptake rate of $90 \mu\text{m min}^{-1}$. Pb mass bias was corrected externally using the $^{205}\text{Tl}/^{203}\text{Tl}$ ratio
145 of the spike and an exponential law. The $^{205}\text{Tl}/^{203}\text{Tl}$ used for correction was determined for
146 each analytical session by minimizing the difference in offset between the session average
147 Pb ratios and the Galer (1997) triple spike Pb isotope values. The Tl isotope ratio was
148 calculated to yield the best fit to all the Pb isotope ratios of Galer (1997) simultaneously.
149 During the analytical sessions, the NBS981 standard solution was analysed regularly
150 (n=16). The average ratios were: $^{206}\text{Pb}/^{204}\text{Pb} = 16.941 \pm 0.0024$ (2 sd), $^{207}\text{Pb}/^{204}\text{Pb} = 15.497$
151 ± 0.0012 (2 sd), $^{208}\text{Pb}/^{204}\text{Pb} = 36.715 \pm 0.0039$ (2 sd). Furthermore, a total procedural
152 BHVO-1 was analysed. The $^{206}\text{Pb}/^{204}\text{Pb}$, $^{207}\text{Pb}/^{204}\text{Pb}$, $^{208}\text{Pb}/^{204}\text{Pb}$ ratios obtained were
153 18.687, 15.568 and 38.342, respectively which is in good agreement with the GEOREM

154 accepted value ($^{206}\text{Pb}/^{204}\text{Pb} = 18.692 \pm 0.008$ (2 sd); $^{207}\text{Pb}/^{204}\text{Pb} = 15.572 \pm 0.006$ (2 sd);
155 $^{208}\text{Pb}/^{204}\text{Pb} = 38.355 \pm 0.022$ (2 sd)).

156

157 At Macquarie, Sr was separated from the sample solution using Biorad AG50W-X8 resin
158 and Nd was collected after separation from Ba and LREE using Eichrom[®] Ln.spec resin
159 columns following the method of Pin et al. (1997). $^{87}\text{Sr}/^{86}\text{Sr}$ and $^{143}\text{Nd}/^{144}\text{Nd}$ ratios were
160 measured by TIMS using a Thermo-Fisher Triton instrument. During the analytical session,
161 instrument performance was monitored by analyses of Sr standards NBS987 and Nd
162 standard JMC321 and mass bias was corrected as in Durham. The average $^{87}\text{Sr}/^{86}\text{Sr}$ for
163 NBS987 was 0.710220 ± 0.000022 (2sd, n=4) and the average $^{143}\text{Nd}/^{144}\text{Nd}$ for JMC321
164 was 0.511123 ± 0.000006 (2sd; n=3). $^{87}\text{Sr}/^{86}\text{Sr}$ and $^{143}\text{Nd}/^{144}\text{Nd}$ were not reported relative
165 to a literature value. During the course of this study, analyses of processed international
166 BHVO-2 standard yielded average $^{87}\text{Sr}/^{86}\text{Sr}$ and $^{143}\text{Nd}/^{144}\text{Nd}$ ratios of was $0.703469 \pm$
167 0.000012 (2sd; n=4) and 0.512976 ± 0.000012 (2sd; n=4), respectively.

168 3.2. $^{87}\text{Sr}/^{86}\text{Sr}$ in plagioclase

169 Four of the most continental-like lavas from St Lucia (SVC), ranging from andesitic to
170 dacitic in composition and with very similar whole rock radiogenic isotope signatures, were
171 chosen for in-depth isotopic study. Sr isotope ratios were determined for five single
172 plagioclase crystals from each lava. The crystals were carefully hand-picked from lightly
173 crushed hand specimens using a binocular microscope. Grains were selected for being free
174 of both inclusions and adhering glass. Each grain, containing at least 60 ng Sr, was
175 individually digested in Romil Upa grade HNO_3 and HF. Sr was separated using Sr-spec

176 resin columns and $^{87}\text{Sr}/^{86}\text{Sr}$ was measured by TIMS using the Thermo Fisher Triton at
177 Durham University. During the TIMS analyses, the average $^{87}\text{Sr}/^{86}\text{Sr}$ ratio for NBS987
178 obtained on 12ng of Sr was 0.710243 ± 0.000009 (2sd, n=3). This is in excellent agreement
179 with the value reported by Thirlwall (1991) of 0.710248 ± 0.000023 (2sd, n=427). Two
180 total procedure blanks contained 18 and 32 pg of Sr which represent 0.03 and 0.05% of the
181 lowest sample Sr concentration analysed and are therefore negligible.

182 *3.3. $\delta^{18}\text{O}$ in mineral separates*

183 Samples ranging from typical oceanic arc lavas to the most continental-like composition
184 were selected for individual mineral oxygen isotope extraction by laser-fluorination.
185 Minerals separates were hand-picked from lightly crushed hand specimens under a
186 binocular microscope, avoiding any inclusions or glass adhering to the grains. Oxygen was
187 extracted from 0.9-3.7 mg of separate using a total laser fluorination system based on the
188 method of Sharp (1990), at the Scottish Universities Environmental Research Centre
189 (SUERC). All fluorinations resulted in 100% release of O_2 from mineral lattice. This
190 oxygen was converted to CO_2 and analyzed on a VG Optima mass spectrometer. Oxygen
191 isotope ($\delta^{18}\text{O}$) values are reported as per mil (‰) deviations relative to Vienna Standard
192 Mean Ocean Water (V-SMOW). Samples were analysed during two periods. During the
193 first period (March 2012) 31 unknowns were analysed along with the international and in-
194 house standards UWG2 and SES and GP147. The average $\delta^{18}\text{O}$ values obtained for UWG2
195 (garnet, $+5.7\text{‰} \pm 0.2$ (2sd), n = 11), SES (quartz, $+10.4\text{‰} \pm 0.6$ (2sd), n = 10) and GP147
196 (garnet, $+7.2\text{‰} \pm 0.4$ (2sd), n = 3) are in very good agreement with their accepted values
197 of $+5.8\text{‰}$ (Valley et al., 1995), $+10.2\text{‰}$ and $+7.2\text{‰}$ (Mattey and Macpherson, 1996).
198 respectively. The internal SES standard has been run many hundreds of time over the past

199 20 years in SUERC, and is well calibrated against UWG2, NBS 28 and NBS 30, as well as
200 GP147. Twelve unknowns were analysed during the second period of study (November
201 2012) when the average $\delta^{18}\text{O}$ values for UWG2, SES and GP147 were $+5.9\text{‰} \pm 0.2$ (2 sd,
202 $n = 2$), $+10.2\text{‰} \pm 0.3$ (2 sd, $n = 6$), $+7.15\text{‰} \pm 0.4$ (2 sd, $n = 2$) respectively.

203 **4.Results**

204 Whole rock Sr, Nd and Pb isotope ratios are given in Table 1. Plagioclase Sr isotopes and
205 mineral $\delta^{18}\text{O}$ data are presented in Tables 2 and 3 respectively.

206 Whole rock $^{87}\text{Sr}/^{86}\text{Sr}$ and $^{143}\text{Nd}/^{144}\text{Nd}$ ratios range between 0.70411 and 0.70622 and
207 0.51251 and 0.51298, respectively, in the Pre-SVC samples and from 0.70754 to 0.70906
208 and 0.51210 to 0.51226, respectively, in the SVC samples (Fig. 2a). Whole rock
209 $^{206}\text{Pb}/^{204}\text{Pb}$, $^{207}\text{Pb}/^{204}\text{Pb}$ and $^{208}\text{Pb}/^{204}\text{Pb}$ ratios were analysed in selected samples with the
210 highest and the lowest $^{87}\text{Sr}/^{86}\text{Sr}$ isotope ratios, to verify coupling with other isotopic
211 systems. Pb isotope ratios vary from 19.291 to 19.341 for $^{206}\text{Pb}/^{204}\text{Pb}$, from 15.747 to
212 15.748 for $^{207}\text{Pb}/^{204}\text{Pb}$ (Fig. 2b) and from 38.96 to 39.11 for $^{208}\text{Pb}/^{204}\text{Pb}$ in the Pre-SVC
213 lavas analysed. In the SVC lavas, ratios vary from 19.721 to 19.797 for $^{206}\text{Pb}/^{204}\text{Pb}$, from
214 15.826 to 15.846 for $^{207}\text{Pb}/^{204}\text{Pb}$ and from 39.438-39.528 for $^{208}\text{Pb}/^{204}\text{Pb}$. Plagioclase
215 crystals from the SVC have heterogeneous $^{87}\text{Sr}/^{86}\text{Sr}$ ratios (Fig. 3) ranging between 0.7083
216 and 0.7094 with variations of up to 0.00083 among crystals from a single lava (SL-JL-51).
217 In the Pre-SVC, plagioclase and pyroxene $\delta^{18}\text{O}$ vary from + 6.4 to +7.9‰ and from +6 to
218 +6.8‰ respectively (Fig. 4). In the SVC, mineral $\delta^{18}\text{O}$ are higher and vary from +7.5 to
219 +10.9‰ for plagioclase, from +10.6 to +11.8‰ for quartz, from +9.4 to +9.8‰ for
220 amphibole and +9 to +9.5‰ for pyroxene.

221 **5.Discussion**

222 *5.1.Intra-crustal magma contamination*

223 The unusually radiogenic composition of some lavas from the Lesser Antilles arc has been
224 explored by many authors using whole rock samples, and explained through models
225 invoking either sediment incorporation into the source (e.g. Labanieh et al., 2010) or
226 assimilation during fractional crystallisation (AFC; e.g. Davidson, 1987). Discriminating
227 between these two processes using only whole rock isotopes is difficult mainly due to
228 uncertainties in determining the precise composition of the endmembers. Correlations
229 between whole rock isotopes and indexes of differentiation such as SiO₂ or MgO are
230 however useful in detecting isotopic changes during differentiation and have been
231 employed by several authors to argue for AFC in Grenada (Thirlwall et al., 1996), the
232 Grenadine Islands (Smith et al., 1996) and Martinique (Davidson, 1987; Davidson and
233 Wilson, 2011). In St Lucia, two distinct trends are observed (Fig. 2c): the first one,
234 comprising only some Pre-SVC samples (Pre-SVC1), shows an absence of covariation
235 between radiogenic isotopes and SiO₂ or MgO while the second trend, comprising the
236 remaining Pre-SVC (Pre-SVC2) and the SVC lavas, displays progressive increase in Sr
237 and decrease in Nd isotope ratios with increasing SiO₂ and decreasing MgO. Pb isotope
238 ratios were not analysed for all St Lucia lavas but variations in the Pre-SVC1 and SVC
239 lavas are consistent with those defined by Sr and Nd isotopes (Fig. 2d). While the first
240 (“vertical”) trend can be explained by simple differentiation of a mafic mantle-derived
241 magma, the second trend requires a different/additional process. If this latter trend were to
242 reflect a source process, this would require either (1) the production of silicic SVC magmas
243 in the mantle or (2) their derivation by differentiation of more mafic melts from a mantle

244 source where a common factor controls both the amount of sediment melt/sediment derived
245 fluids added to the source and the future extent of magma differentiation. The first
246 hypothesis cannot be reconciled with the low MgO content of silicic SVC lavas
247 compositions (MgO = 1.1-2.7 wt.%) since andesitic to dacitic magma generated either by
248 mantle melting or by reaction between ascending slab-derived silicic melts and mantle
249 peridotite typically have elevated MgO contents (Grove et al., 2003; Yogodzinsky and
250 Kelemen, 1998). The second hypothesis, involving a coincidental process, is equally very
251 hard to conceive. It is, however, directly testable. Since magmatic differentiation has
252 negligible effect on radiogenic isotopic ratios, the amount of sediment incorporated into
253 the magma during its genesis in the mantle should be reflected in the $^{87}\text{Sr}/^{86}\text{Sr}$ of all its
254 components. Therefore, once separated from its source, a magma that has remained a
255 closed system should demonstrate negligible $^{87}\text{Sr}/^{86}\text{Sr}$ variation between the melt and all
256 phenocrysts. Furthermore, the Sr isotope ratio of the phenocrysts would also be observed
257 for the whole rock. Conversely, isotopic disequilibrium between different phases in a rock
258 or between different crystals of the same phase would require that open system behaviour
259 occurred. Therefore, the variation in $^{87}\text{Sr}/^{86}\text{Sr}$ ratios within single samples is a hallmark
260 for open system behaviour (Davidson et al., 2007).

261 Despite their similar whole rock Sr isotopic ratios, the $^{87}\text{Sr}/^{86}\text{Sr}$ ratios of crystals from the
262 four SVC samples vary substantially amongst and within hand specimens (Table 2; Fig.3).
263 Such disequilibrium cannot be explained by incorporation of sediment in the source, and
264 must instead be accounted for by an open system process, such as crustal assimilation
265 during crystallisation.

266 Most of the plagioclase crystals analysed have lower $^{87}\text{Sr}/^{86}\text{Sr}$ than their respective whole
267 rock values. This indicates that at least part of the volume of each of those plagioclase
268 crystals grew in a magma with less radiogenic Sr than now represented by the matrix. The
269 zoned nature of the crystals requires an igneous origin but does not allow discrimination
270 between phenocrysts which grew from a magma changing in $^{87}\text{Sr}/^{86}\text{Sr}$ composition and
271 xenocrysts which were remobilized during re-melting of plutonic rocks. The latter option
272 was preferred by Schmitt et al. (2010) to explain variation in core to rim U-Th zircon ages
273 obtained in the SVC lavas.

274 *5.2. Effect of contamination on whole rock compositions*

275 In order to confirm that crustal assimilation is largely responsible for the radiogenic whole
276 rock isotopic signatures observed in St Lucia, the mineral $\delta^{18}\text{O}$ study was performed.
277 Although the $\delta^{18}\text{O}$ of crustal-derived material ($> +10\text{‰}$) is much higher than the mantle
278 range ($+ 5.5\text{‰} \pm 0.2$), 80% of the $\delta^{18}\text{O}$ values of any given phase in oceanic arc lavas fall
279 within $\pm 0.2\text{‰}$ of the average value for that phase in upper mantle peridotites and MORBs
280 (Eiler et al., 2000; Matthey et al., 1994). Because the concentration of oxygen in the mantle
281 and the crust is similar, a large input of crustal derived fluids and/or sediments would be
282 necessary to modify the mantle signature (James, 1981). Thus, O isotopes provide a
283 powerful tool to discriminate between addition of sediments to the mantle source from
284 assimilation of sediments in the arc crust, the latter being a much more efficient way of
285 modifying the mantle-derived $\delta^{18}\text{O}$ value of the magma (e.g. Macpherson et al., 1998).
286 Previous oxygen isotopic analyses performed on olivine and pyroxene phenocrysts from
287 the Lesser Antilles showed the existence of values greater than the mantle range and that

288 these correlate with whole rock radiogenic isotopes, suggesting crustal assimilation (Smith
289 et al., 1996; Thirlwall et al., 1996; Van Soest et al., 2002). However, although higher, the
290 excess relative to the range of mantle $\delta^{18}\text{O}$ values was small, with only up to + 1‰ excess
291 for olivine and up to + 0.6‰ for pyroxene with the exception of one pyroxene, which was
292 + 1.6‰ and two quartz crystals which were + 3.83‰ and + 4.37‰ higher than the mantle
293 range.

294 In this study, 93% of the 44 mineral analyses lie outside their respective mantle ranges and
295 the SVC displays extreme $\delta^{18}\text{O}$ values never observed before in oceanic arcs lacking
296 known continental basement (Fig.4). Moreover, a strong positive correlation is observed
297 between the mineral $\delta^{18}\text{O}$ and the whole rock radiogenic isotopes (Fig. 5) with the highest
298 $\delta^{18}\text{O}$ values found in SVC lavas with very radiogenic whole rock $^{87}\text{Sr}/^{86}\text{Sr}$ and
299 $^{206,207,208}\text{Pb}/^{204}\text{Pb}$ ratios (and unradiogenic $^{143}\text{Nd}/^{144}\text{Nd}$ ratios). Although the SVC products
300 have more differentiated compositions than the pre-SVC samples, the maximum effect of
301 closed system differentiation on $\delta^{18}\text{O}$ is typically very small: +0.3 to +0.4‰ (Bindeman et
302 al., 2004; Macpherson and Matthey, 1998). Thus, even after correction for this effect, the
303 SVC mineral $\delta^{18}\text{O}$ range lies well beyond the mantle range. The mean anorthite (An)
304 content of SVC plagioclase is slightly lower than that of the pre-SVC crystals. However,
305 since the difference is small (mean An of 68% (ranging from 65% to 71%) and of 59%
306 (ranging from 54% to 68%) respectively for SVC andesite and dacite vs. mean An of 80%
307 (70% - 90%) for Pre-SVC basaltic andesite and basalt) the related increase in $\delta^{18}\text{O}$ in the
308 SVC plagioclase is thought to be negligible. This is confirmed by the fact that phenocrysts
309 from SVC lavas with different SiO_2 (high-silica andesites and dacites: 60.5 – 67.5 wt. %)
310 possess similar $\delta^{18}\text{O}$ values. SVC plagioclase-quartz pairs (from the same hand sample)

311 have $\Delta_{\text{plag-qtz}}$ (where $\Delta_{i-j} = \delta^{18}\text{O}_i - \delta^{18}\text{O}_j$) between -0.1 to -1.21 ‰ (n = 8; with n=5 higher
312 than -0.7‰) except for one pair where $\Delta_{\text{plag-qtz}} = -3.9$ ‰. Andesitic-dacitic temperatures
313 (T= 800-1000°C) typically produce $\Delta_{\text{plag-qtz}}$ between -0.84 and -1.45 ‰ (e.g. using the
314 Chiba et al. (1989) fractionation coefficients and considering a large range of anorthite
315 content between An₄₀ and An₇₀). Therefore, most $\Delta_{\text{plag-qtz}}$ are higher than equilibrium. SVC
316 plagioclase-pyroxene pairs display fractionation of $\Delta_{\text{plag-py}}$ between +0.60 and +0.95 ‰
317 (n=3) which are similar to that expected from equilibrium fractionation at andesitic-dacitic
318 temperatures ($\Delta_{\text{plag-py}} = +0.66$ to $+1.21$ ‰ at T° = 800-1000 and An₄₀₋₇₀). Therefore, both
319 pyroxene and plagioclase are likely to have crystallized in equilibrium from a similar
320 magma. The lowest $\delta^{18}\text{O}$ values are observed in Pre-SVC1 lavas, which have low whole
321 rock $^{87}\text{Sr}/^{86}\text{Sr}$ and Pb isotope ratios (SL-83-25, 44). In these samples, $\delta^{18}\text{O}_{\text{plag}}$ values are
322 higher than the mantle range, whereas the $\delta^{18}\text{O}_{\text{px}}$ values overlap the upper end of the mantle
323 range. However, plagioclase-pyroxene pairs ($\Delta_{\text{plag-py}}$ from +0.3 to +0.6 ‰) are close to
324 oxygen isotopic equilibrium at basaltic to basaltic andesite temperatures ($\Delta_{\text{plag-py}} = +0.35$
325 ‰ to +0.51‰ at T° = 1100-1200°C and An₉₉₋₈₀ using Chiba et al.'s (1989) equation). Thus,
326 it is difficult, in these samples, to differentiate between small error on the mantle mineral
327 range of composition and the impact of small amounts of crustal assimilation during
328 plagioclase crystallization. Pre-SVC2 lavas, that have the highest whole rock $^{87}\text{Sr}/^{86}\text{Sr}$
329 ratios (SL-83-26; $^{87}\text{Sr}/^{86}\text{Sr} = 0.706219$; basaltic andesite) of the Pre-SVC group, also
330 display higher $\delta^{18}\text{O}_{\text{plag}}$ than $\delta^{18}\text{O}_{\text{px}}$. However, $\Delta_{\text{plag-py}}$ varies between +0.5 ‰ to +1.5 ‰.
331 Such values are too high to be explained simply by equilibrium fractionation. We believe
332 that the high $\Delta_{\text{plag-py}}$ values result from the addition of a crustal component late in the
333 differentiation sequence when plagioclase formed a larger component of the crystallising

334 assemblage. This provides further support for an origin through crustal assimilation rather
335 than sediment addition to the source. In this case, plagioclase provides a more sensitive
336 record of crustal assimilation than the mafic phases. This may be important when targeting
337 minerals for oxygen isotopic analysis in settings where more subtle changes in $\delta^{18}\text{O}$ are
338 anticipated, due to smaller isotopic contrasts between magma and the crust into which it is
339 emplaced.

340 A simple mixing model (Fig. 5) between a typical mantle composition and a sediment
341 having the highest $\delta^{18}\text{O}$ reported (+ 35 ‰; Bindeman, 2008) shows that a minimum of 10-
342 20 % of sediment would be required to be added to the mantle or a mantle derived magma
343 in order to explain the SVC mineral $\delta^{18}\text{O}$ data. However, we know from DSDP 78A site
344 543 and DSDP 14 site 144 that sediments subducted at the Lesser Antilles trench comprise
345 a mixture of pelagic clay, radiolarian clay, terrigenous claystone siltstone and sandstones
346 (30% carbonate on average; Carpentier et al., 2008). Thus, the bulk sediment would possess
347 an average $\delta^{18}\text{O}$ closer to the composition of site 543 pelagic clays of +20‰ (Davidson,
348 1987). In this more realistic case, addition of 20-40% sediment would be required to
349 generate the range of SVC $\delta^{18}\text{O}$ values and addition of 10-20% sediment could reproduce
350 the Pre-SVC sample with the most elevated $\delta^{18}\text{O}_{\text{plag}}$ (+7.3 to +7.9‰ in SL-83-26; Fig. 5c).
351 Introducing such large amounts of sediments to the mantle wedge should also modify the
352 major element composition of the primitive magmas, such that increasing sediment
353 incorporation (i.e. increasing mineral $\delta^{18}\text{O}$ and $^{87}\text{Sr}/^{86}\text{Sr}$) should correlate with an increase
354 of SiO_2 (clay, sand) or CaO (carbonate) of the melt. As discussed in section 5.1., the SVC
355 lavas cannot have been directly produced in the mantle since their MgO is too low. If the
356 SVC lavas resulted from differentiation of a primary magma produced in the mantle by

357 mixing with substantial amounts of sediment melt, the resulting suite of lava would likely
358 have a higher SiO₂ or CaO content than a suite derived from Pre-SVC_{1,2} primitive magmas
359 at a given MgO content (different differentiation trends). However, SVC and Pre-SVC_{1,2}
360 lavas share similar (although scattered) differentiation trend (Fig. 6), and therefore back
361 project toward a similar primitive magma. Hence, it seems unlikely that the SVC and Pre-
362 SVC lavas were derived from very different mantle sources. Instead, the single trend of
363 differentiation recorded by major elements in all St Lucia lavas is consistent with variable
364 assimilation of crustal material. This is because, during differentiation, major element
365 compositions are largely controlled by phase equilibria and, to a lesser extent, by the nature
366 of the sediment assimilated, the latter likely to be derived from the erosion of upper
367 continental crust with a similar composition to the felsic differentiates of the Pre-SVC lavas
368 (Fig. 6). Therefore, the strong correlation between $\delta^{18}\text{O}$ and whole rock Sr isotopes indicate
369 that assimilation is the major factor controlling the whole rock radiogenic isotope ratios
370 observed in the St Lucia lavas (Fig.7). For both plagioclase and pyroxene, the correlation
371 is slightly convex-up, suggesting that the magma had a slightly lower Sr content than the
372 material it assimilated (c.f. inset to Fig.5). More importantly, the plagioclase $\delta^{18}\text{O}$ values
373 are displaced further from the mantle field than is the case for pyroxene in Pre-SVC
374 samples, requiring a larger proportion of assimilant than required for the pyroxenes. Quartz
375 is only found in the SVC lavas where no correlation between $\delta^{18}\text{O}_{\text{qz}}$ and whole rock
376 $^{87}\text{Sr}/^{86}\text{Sr}$ is observed. The slight disequilibrium between quartz and plagioclase (low $\Delta_{\text{plag-}}$
377 qtz) indicates that quartz crystallized in a magma with slightly lower $\delta^{18}\text{O}$ than the
378 plagioclase.

379 *5.3. Implications for other Lesser Antilles volcanoes and other arcs*

380 The crystal $^{87}\text{Sr}/^{86}\text{Sr}$ data show that lavas with extreme whole rock compositions underwent
381 assimilation of crustal material in an open system supporting previous work by Davidson
382 (1987), Davidson and Harmon (1989) Smith et al. (1996), Thirwall et al. (1996), Thirlwall
383 and Graham (1984) and Van Soest et al. (2002). The extreme $\delta^{18}\text{O}$ signature observed in
384 lavas with the most continental Sr, Nd and Pb isotope ratios (SVC) confirms late
385 assimilation of arc crust as the cause of these variations and shows that the amount of
386 material assimilated is not trivial ($>20\%$). More importantly, crustal assimilation did not
387 only affect the andesites and dacites, but also substantially (10-20% assimilation) modified
388 the composition of a basaltic andesite (Pre-SVC2) with similar SiO_2 and MgO contents to
389 the most mafic lava of the island. Therefore, in St Lucia, the use of the most mafic lavas
390 erupted on the island to constrain the source characteristics is compromised since some of
391 them have clearly interacted with the crust. Similar problems may affect other Lesser
392 Antilles islands and other oceanic arcs where basaltic andesites with MgO ~ 4 wt. %, or
393 even more differentiated lavas, have been used studies to constrain the source composition.
394 For example Labanich et al. (2010) suggested that isotopic ratios in lavas from Martinique
395 with up to ~ 70 wt. % SiO_2 (MgO ~ 0.23) faithfully reflect the source composition.
396 Likewise, Carpentier et al. (2008) modeled all the published data for Lesser Antilles lavas
397 by sediment addition to the source, without taking into account the degree of differentiation
398 of the lavas.

399 Because St Lucia lavas encompass Sr, Nd and Pb isotopic range almost as great as the
400 whole Lesser Antilles arc it follows that much of the isotopic heterogeneity observed in the
401 rest of the arc could also reflect variable crustal assimilation. Sediment present in the Lesser
402 Antilles arc crust is likely to originate from the closest continental mass: South America.

403 It has very “continental” $^{87}\text{Sr}/^{86}\text{Sr}$, $^{143}\text{Nd}/^{144}\text{Nd}$ and $^{206,207,208}\text{Pb}/^{204}\text{Pb}$ ratios (e.g. Carpentier
404 et al., 2008). Sediments with such signatures were found on the edge of the north east part
405 of South America (site 144 sediment; Carpentier et al.(2008, 2009)) and their presence on
406 the subducting plate was used as a strong argument for incorporation of sediment in the
407 mantle source as being the cause for the extreme isotopic compositions of the arc lavas.
408 However, our data show that most of the arc lava isotopic variations are generated by
409 contamination in the arc crust. Therefore, subduction of material resembling site 144
410 sediments is not *required* to explain the extreme Sr, Nd, Pb and O isotopic signatures of
411 the Lesser Antilles arc lavas.

412

413 It is important to stress that this does not preclude incorporation of subducted sediment into
414 the source of the lavas having an impact on the whole rock isotopic ratios. Indeed, mineral
415 $\delta^{18}\text{O}$ compositions of the Pre-SVC1 lavas (SL-83-44; SL-83-25) are very close to mantle
416 values which indicate that, if crustal assimilation affected these lavas, it would be in very
417 low amounts. Yet, although their Sr and Nd isotope ratio overlap typical oceanic arc
418 compositions, their Pb isotope ratios are slightly more radiogenic (Fig. 2b). This not only
419 suggests the involvement of sediment in the source but also that these are slightly more
420 abundant or more radiogenic than sediments present in the source of most “typical” oceanic
421 arcs. However, Sr, Nd and Pb isotope compositions of the Pre-SVC1 lavas remain very
422 close to typical oceanic composition spectrum, and we suggest that subducted material is
423 not a major factor in causing large isotopic heterogeneity in Lesser Antilles arc lavas.

424 The extreme contamination observed in at least some of the Lesser Antilles lavas may
425 reflect the unique presence of sediment in the arc crust that, in turn, reflects a specific
426 geodynamic context (Aitken et al., 2011). However, similar assimilation of sediments
427 and/or altered crust in lower amounts and/or different composition may occur in other
428 oceanic arcs and has already been suggested to explain compositions observed in the
429 offshore Taupo Volcanic zone in New Zealand (Macpherson et al., 1998). Eiler et al. (2000)
430 estimated that although most oceanic arc minerals (olivine, plagioclase, glass, biotite) fall
431 within the mantle range in $\delta^{18}\text{O}$, around 20% of the data are slightly higher by up to 0.43‰.
432 These 'out of mantle range' phases come from samples with higher whole rock Sr isotope
433 ratios, which is also what we observe on St Lucia. Because the displacement from the
434 mantle range is not substantial, these data have been interpreted to reflect sediment
435 incorporation into the mantle wedge. However, all these higher $\delta^{18}\text{O}$ ratios were observed
436 in mafic minerals (primarily olivine). At St Lucia, in the least contaminated rocks,
437 plagioclase reveals assimilation more clearly than pyroxene, probably because it
438 crystallised over a greater range of magmatic evolution, persisting to the most
439 differentiated stages. Hence, comparing olivine and pyroxene $\delta^{18}\text{O}$ values with whole rock
440 $^{87}\text{Sr}/^{86}\text{Sr}$ may be a less effective means to detect small amounts of assimilation than the use
441 of plagioclase $\delta^{18}\text{O}$ data.

442 **6. Summary and conclusions**

443 Our new single plagioclase Sr isotopic data and mineral $\delta^{18}\text{O}$ data show that crustal
444 assimilation was important in magma evolution at St Lucia. Correlations of mineral $\delta^{18}\text{O}$
445 values with whole rock Sr isotopic composition shows that assimilation controls most of
446 the Sr, Nd and Pb isotopic variation in St Lucia lavas. Isotopic variation at St. Lucia

447 replicates most of the range for the whole Lesser Antilles arc, therefore we suggest that up
448 to 20-40% assimilation could be responsible for the unusual diversity of isotopic
449 compositions observed along the arc. Assimilation of such large volumes of sediment
450 within the Lesser Antilles crust may be related to a specific geographic and geodynamic
451 setting. However, similar crustal assimilation could take place in other oceanic arcs where
452 a lack of geochemical contrast between assimilated sediments and the magma and/or the
453 lower amounts of sediments assimilated may make it more challenging to track.

454 **Acknowledgements**

455 Financial support was provided to Rachel Bezard by Durham and Macquarie University
456 cotutelle studentship. AJB is funded by NERC support of the Isotope Community Support
457 Facility at SUERC. O isotope analyses were possible due to a NERC Facilities award to
458 JPD (IP-1285-1111). We thank Geoff Nowell for guidance during whole rock isotope work
459 and micro-Sr analytical work at Durham University; Peter Wieland for his help during
460 whole rock isotope work at Macquarie University; Alison McDonald and Terry Donnelly
461 for their help with the O isotope analyses. The paper has greatly benefited from comments
462 by two anonymous reviewers and by the editor, Tim Elliott.

463 **References**

- 464 Annen, C., Blundy, J.D. and Sparks, R.S.J., 2006. The Genesis of Intermediate and silicic
465 magmas in deep crustal hot zones. *J. Petrology* 47, 505-539.
- 466 Aitken, T., Mann, P., Escalona, A., Christeson, G.L., 2011. Evolution of the Grenada and
467 Tobago Basins and implications for arc migration. *Mar. Petrol. Geol.* 28, 235-258.

468 Bindeman, I., 2008. Oxygen Isotopes in Mantle and Crustal Magmas as Revealed by Single
469 Crystal Analysis. *Rev. Mineral. Geochem.* 69, 445-478.

470 Bindeman, I.N., Valley, J.W., 2002. Oxygen isotope study of the Long Valley magma
471 system, California: isotope thermometry and convection in large silicic magma bodies.
472 *Contrib. Mineral. Petrol.* 144, 185-205.

473 Bindeman, I.N., Ponomareva, V.V., Bailey, J.C., Valley, J.W., 2004. Volcanic arc of
474 Kamchatka: a province with high- $\delta^{18}\text{O}$ magma sources and large-scale $^{18}\text{O}/^{16}\text{O}$ depletion
475 of the upper crust. *Geochim. Cosmochim. Acta* 68, 841-865.

476 Briden, J.C., Rex, D.C., Faller, A.M., Tomblin, J.F., 1979. K-Ar geochronology and
477 paleomagnetism of volcanic rocks in the Lesser Antilles island arc. *Philos. Trans. R. Soc.*
478 *Lond. A Math. Phys. Eng. Sci.* 291, 485-528.

479 Carpentier, M., Chauvel, C., Mattielli, N., 2008. Pb–Nd isotopic constraints on
480 sedimentary input into the Lesser Antilles arc system. *Earth Planet. Sci. Lett.* 272, 199-
481 211.

482 Carpentier, M., Chauvel, C., Maury, R.C., Mattielli, N., 2009. The ‘Zircon effect’ as
483 recorded by the chemical and Hf isotopic composition of Lesser Antilles forearc sediments.
484 *Earth Planet. Sci. Lett.* 287, 86-99.

485 Chazot, G., Lowry, D., Menzies, M., Matthey, D., 1997. Oxygen isotopic composition of
486 hydrous and anhydrous mantle peridotites. *Geochim. Cosmochim. Acta* 61, 161-169.

487 Chiba, H., Chacko, T., Clayton, R.N., Goldsmith, J.R., 1989. Oxygen isotope fractionations
488 involving diopside, forsterite, magnetite, and calcite: Application to geothermometry.
489 *Geochim. Cosmochim. Acta* 53, 2985-2995.

490 Davidson, J. P., 1986. Isotopic and trace element constraints on the petrogenesis of
491 subduction-related lavas from Martinique, Lesser Antilles. *J. Geophys. Res.* 91, 5943-
492 5962.

493 Davidson, J.P., 1987. Crustal contamination versus subduction zone enrichment: example
494 from the lesser antilles and implications for mantle source compositions of island arc
495 volcanic rocks. *Geochim. Cosmochim. Acta* 51, 2185-2198.

496 Davidson, J.P., Harmon, R.S., 1989. Oxygen isotope constraints on the petrogenesis of
497 volcanic arc magmas from Martinique, Lesser Antilles. *Earth Planet. Sci. Lett.* 95, 255-
498 270.

499 Davidson, J.P., Morgan, D.J., Charlier, B.L.A., Harlou, R., Hora, J. M., 2007.
500 Microsampling and isotopic analysis of igneous rocks: implications for the study of
501 magmatic systems. *Annu. Rev. Earth Planet. Sci.* 35, 273-311.

502 Davidson, J.P., Wilson, M., 2011. Differentiation and Source Processes at Mt Pelée and
503 the Quill; Active Volcanoes in the Lesser Antilles Arc. *J. petrology* 52, 1493-1531.

504 De Kerneizon, M.L., Bellon, H., Carron, J.P., Maury, R.C., 1983. The island of St-Lucia-
505 petrochemistry and geochronology of the main magmatic series. *Bull. Soc. Géol. Fr.* 25,
506 845-853.

507 Eiler, M.J., Crawford, A., Elliott, K.A.F., Valley, J.W. and Stolper, E.M., 2000. Oxygen
508 Isotope Geochemistry of Oceanic-Arc Lavas. *J. petrology* 41, 229-256.

509 Grove, T.L., Elkins-Tanton, L.T., Parman, S.W., Chatterjee, N., Muntener, O., Gaetani,
510 G.A., 2003. Fractional crystallisation and mantle melting controls on calc-alkaline
511 differentiation trends. *Contrib. Mineral. Petrol.* 145, 515-533.

512 James, D.E., 1981. The combined use of oxygen and radiogenic isotopes as indicators of
513 crustal contamination. *Annu. Rev. Earth Planet. Sci.* 9, 311-344.

514 Heath, E., Macdonald, R., Belkin, H., Hawkesworth, C., Sigurdsson, H., 1998.
515 Magmagenesis at Soufriere Volcano, Lesser Antilles Arc. *J. Petrology* 39, 1721-1764.

516 Labanieh, S., Chauvel, C., Germa, A., Quidelleur X., Lewin E., 2010. Isotopic hyperbolas
517 constrain sources and processes under the Lesser Antilles arc. *Earth Planet. Sci. Lett.* 298,
518 35-46.

519 Labanieh, S., Chauvel, C., Germa, A., Quidelleur, X., 2012. Martinique: a clear case for
520 sediment melting and slab dehydration as a function of distance to the trench. *J. Petrology*
521 53, 2441-2464.

522 Lindsay, J.M., Trumbull, R.B., Schmitt, A.K., Stockli, D.F., Shane, P., Howe, T., 2013.
523 Volcanic stratigraphy and geochemistry of the Soufrière Volcanic Center, Saint Lucia with
524 implications for volcanic hazards. *J. Volcanol. Geoth. Res.* doi:
525 10.1016/j.jvolgeores.2013.04.011.

526 Macdonald, R., Hawkesworth, C.J., Heath, E., 2000. The Lesser Antilles volcanic chain: a
527 study in arc magmatism. *Earth-Sci. Rev.* 49, 1-76.

528 Macpherson, C.G., Matthey, D.P., 1998. Oxygen isotope variations in Lau Basin basalts.
529 Chem. Geol. 144, 177-194.

530 Macpherson, C.G., Gamble, J.A., Matthey, D.P., 1998. Oxygen isotope geochemistry of lavas
531 from an oceanic to continental arc transition, kermadec-Hikurangi margin, SW Pacific.
532 Earth Planet. Sci. Lett. 160, 609-620.

533 Matthey, D.P., Macpherson, C., 1993. High-precision oxygen isotope microanalysis of
534 ferromagnesian minerals by laser fluorination. Chem. Geol., 105, 305-318.

535 Matthey, D.P., Lowry, D., Macpherson, C., 1994. Oxygen isotope composition of mantle
536 peridotite. Earth Planet. Sci. Lett. 128, 231-241.

537 Nowell, G., Parrish, R.R., 2001. Simultaneous acquisition of isotope compositions and
538 parent/daughter ratios by non-isotope dilution solution-mode plasma ionisation multi-
539 collector mass spectrometry (PIMMS). In: Plasma Source Mass Spectrometry: The New
540 Millennium. Roy. Geol. Soc. Lond. 267, 305 pp.

541 O'Neil, J.R., Chappell, B.W., 1977. Oxygen and hydrogen isotope relations in the Berridale
542 batholiths. J. Geol. Soc. 133, 559-571.

543 Pin, C., Francisco, J., Zalduegui, S. 1997. Sequential separation of light rare-earth
544 elements, thorium and uranium by miniaturized extraction chromatography: Application
545 to isotopic analyses of silicate rocks. Anal. Chim. Acta 339, 79-89.

546 Royse, K., Kempton, P., Darbyshire, D.P.F. 1998. Procedure for the analysis for Rubidium-
547 Strontium and Samarium-Neodymium isotopes at the NERC Isotope Geosciences
548 Laboratory. NERC Isot. Geosc. Lab. Rep. Series 121.

549 Samper, A., Quidelleur, X., Boudon, G., Le Friant, A., Komorowski, J.C., 2008.
550 Radiometric dating of three large volume flank collapses in the Lesser Antilles Arc. *J.*
551 *Volcanol. Geoth. Res.* 176, 485-492.

552 Schmitt, A.K., Stockli, D.F., Lindsay, J.M., Robertson, R., Lovera, O.M., Kislitsyn, R.,
553 2010. Episodic growth and homogenization of plutonic roots in arc volcanoes from
554 combined U-Th and (U-Th)/He zircon dating. *Earth Planet. Sci. Lett.* 295, 91-103.

555 Sharp, Z.D., 1990. A laser-based microanalytical method for the in situ determination of
556 oxygen isotope ratios in silicates and oxides. *Geochim. Cosmochim. Acta* 54, 1353-1357.

557 Sherman, S.B., 1992. Geochemistry and petrogenesis of Saba, Lesser Antilles, [MSc.
558 thesis]. University of South Florida, Tampa. 114 pp.

559 Smith, T.E., Thirlwall, M.F., Macpherson, C., 1996. Trace element and isotope
560 geochemistry of the volcanic rocks of Bequia, Grenadine Island, Lesser Antilles Arc: a
561 study of subduction enrichment and intra-crustal contamination. *J. Petrology* 37, 117-143.

562 Tatsumi, Y., Eggins, S., 1995. *Subduction Zone Magmatism*. Oxford: Blackwell Scientific.

563 Thirlwall, M.F., 1991. Long-term reproducibility of multicollector Sr and Nd isotope ratio
564 analysis. *Chem. Geol.* 94, 85-104.

565 Thirlwall, M. F., Graham, A. M., 1984. Evolution of high-Ca, high-Sr C-series basalts from
566 Grenada, Lesser Antilles: Contamination in the arc crust. *J. Geol. Soc. Lond.* 141, 427-445.

567 Thirlwall, M.F., Graham, A.M., Arculus, R.J., Harmon, R.S., Macpherson, C.G., 1996.
568 Resolution of the effects of crustal contamination, sediment subduction, and fluid transport

569 in island arc magmas: Pb-Sr-Nd-O isotope geochemistry of Grenada, Lesser Antilles.
570 *Geochim. Cosmochim. Acta* 60, 4785-4810.

571 Toothill, J., Williams, C.A., Macdonald, R., Turner, S.P., Roger, N.W., Hawkesworth, C.J.,
572 Jerram, D.A., Ottley, C.J., and Tindle, A.G., 2007. A complex petrogenesis for an arc
573 magmatic suite, St Kitts, Lesser Antilles. *J. Petrology* 48, 3-42.

574

575 Valley, J.W., Kitchen, N., Kohn, M.J., Niendorf, C.R., Spicuzza, 1995. UWG-2, a garnet
576 standard for oxygen isotope ratios: Strategies for high precision and accuracy with laser
577 heating. *Geochim. Cosmochim. Acta* 59, 5223-5231.

578

579 Van Soest, M.C., Hilton, D.R., Macpherson, C.G., Matthey, D.P., 2002. Resolving sediment
580 subduction and crustal contamination in the Lesser Antilles arc: a combined He-O-Sr
581 Isotope approach. *J. Petrology* 43, 143-170.

582 White, W.M., Dupré, B., 1986. Sediment Subduction and Magma Genesis in the Lesser
583 Antilles: Isotopic and Trace Element Constraints. *J. Geophys. Res.* 91, 5927-5941.

584 Yogodzinsky, G.M., Kelemen, P.B., 1998. Slab melting in the Aleutians: implications of
585 an ion probe study of clinopyroxene in primitive adakite and basalt. *Earth Planet. Sci. Lett.*
586 158, 53-65.

587 Ysaccis, R., 1997. Tertiary evolution of the northeastern Venezuela offshore. Ph.D. thesis,
588 Rice University, Houston. 285 pp.

589 **Figure captions**

590 Figure 1: Bathymetric map of the Lesser Antilles arc showing the islands, the trench-
591 deformation front, the main ridges, the Grenada and Tobago basins and the locations of
592 Deep Sea Drilling Project (DSDP) hole 543/543A and hole 144. Figure modified from Van
593 Soest et al. (2002).

594 Figure 2: Whole rock compositions of St Lucia lavas. (a) Sr and Nd and (b) Pb and Nd
595 isotopic diversity. St Lucia data show a similar range to most of the Lesser Antilles arc,
596 ranging between typical oceanic arc compositions and Atlantic sediments cored at the front
597 of the trench (DSDP sites 144 and 543; Carpentier et al., 2008, 2009). SVC = Soufriere
598 Volcanic Complex. Pre-SVC lavas with typical oceanic arc compositions, called Pre-
599 SVC1, are shown by open circles and lavas with the most radiogenic compositions, called
600 Pre-SVC2, are represented by striped circles. The SVC lavas are shown by solid red circles.
601 (b) $^{87}\text{Sr}/^{86}\text{Sr}$ and (d) $^{207}\text{Pb}/^{204}\text{Pb}$ vs. SiO_2 (wt. %) of St Lucia lavas showing the two trends
602 observed. SiO_2 and Sr-Nd-Pb isotopic compositions are provided in the Table 1. Tonga,
603 South Sandwich, Mariana and Aleutian compositions from Georock database:
604 <http://georoc.mpch-mainz.gwdg.de/georoc/>. MORB field is mid-Atlantic Ridge between
605 30°N and 30°S (data from PETDB: <http://petdb.org/science.jsp/>) and the Lesser Antilles
606 arc field represents data from other islands: Grenada from Thirlwall and Graham (1984);
607 Soufrière, St Vincent from Heath et al. (1998); Dominica and Martinique from Davidson
608 (1986, 1987) and Davidson and Wilson (2011); Mt Misery, St Kitts from Toothill et al.
609 (2007), The Quill, Statia from Davidson and Wilson (2011); Saba from Sherman (1992).

610

611 Figure 3: $^{87}\text{Sr}/^{86}\text{Sr}$ isotope ratios of twenty plagioclase phenocrysts showing isotopic
612 disequilibrium among four of the most contaminated SVC lavas. The whole rock value for

613 each lava is shown as a horizontal line. For all data, 2 standard errors (SE) are < 0.000014
614 which is smaller than the symbol size. Data are presented in Table 2.

615 Figure 4: $\delta^{18}\text{O}$ values of phenocrysts from SVC and Pre-SVC lavas (symbols as in Fig.2).
616 Plag = plagioclase; Qz = quartz, Py = pyroxene; Am = amphibole and MA = mantle range.
617 Mantle ranges are from Bindeman and Valley (2002) for Quartz (from differentiation of
618 mantle derived magma), Chazot et al. (1997) for pyroxene and amphibole and Eiler et al.
619 (2000) for plagioclase (defined using crystals from samples with SiO_2 similar to Pre-SVC
620 mafic lavas). 2 sd reproducibility error of the O isotope technique was typically $\pm 0.4 \text{ ‰}$
621 (see section 3.3).

622 Figure 5: Correlation between mineral $\delta^{18}\text{O}$ and whole rock $^{87}\text{Sr}/^{86}\text{Sr}$ and SiO_2 (symbols as
623 in Fig. 2). (a,b) plagioclase and pyroxene $\delta^{18}\text{O}$ vs. whole rock $^{87}\text{Sr}/^{86}\text{Sr}$. (c,d) plagioclase
624 and pyroxene $\delta^{18}\text{O}$ vs. whole rock SiO_2 . Mixing models between mantle ($\delta^{18}\text{O} = +5.7 \text{ ‰}$)
625 and sediment with $\delta^{18}\text{O}$ of $+20 \text{ ‰}$ (1) and $+35 \text{ ‰}$ (2) are also shown. Oxygen concentration
626 is assumed to be the same for both the mantle and the sediment in the model. MA = MORB
627 mantle range with $\delta^{18}\text{O}$ from Eiler et al. (2000) and $^{87}\text{Sr}/^{86}\text{Sr}$ from mid-Atlantic Ridge
628 between 30°N and 30°S (data from PETDB: <http://petdb.org/science.jsp/>). In the schematic
629 inset $[\text{Sr}]_C$ is the Sr concentration in sediment and $[\text{Sr}]_M$ is the Sr concentration in the
630 mantle during source contamination (SC) and in the melt during crustal assimilation (CA).

631 Figure 6: Variation of SiO_2 and CaO with MgO composition with the Pre-SVC and SVC
632 lavas. Upper continental crust composition is from Rudnick and Fountain (1995). The
633 schematic inset illustrates the impact of incorporation of large amounts of terrigenous

634 sediment into the mantle source on primitive magma compositions. The same concept can
635 be applied to CaO versus MgO, for large amounts of carbonate rich sediment.

636 Figure 7: Schematic model for the St Lucia magmatic plumbing system through time to
637 explain the Pre-SVC and SVC whole rock and mineral isotopic compositions. The bottom
638 panel illustrates the storage, intrusion and eruption of the Pre-SVC lavas. The magma
639 storage is limited and/or occurs mostly in the mantle and in the oceanic crust: assimilation
640 of sediment (purple) is limited. The middle panel illustrates the development of a large
641 SVC andesitic complex at shallower depth where active assimilation of sediment takes
642 place. Finally, the upper panel illustrates the evolution of the SVC dacite from the andesite.
643 Minimal or no assimilation occurs at this stage.

Fig. 1



Fig. 2

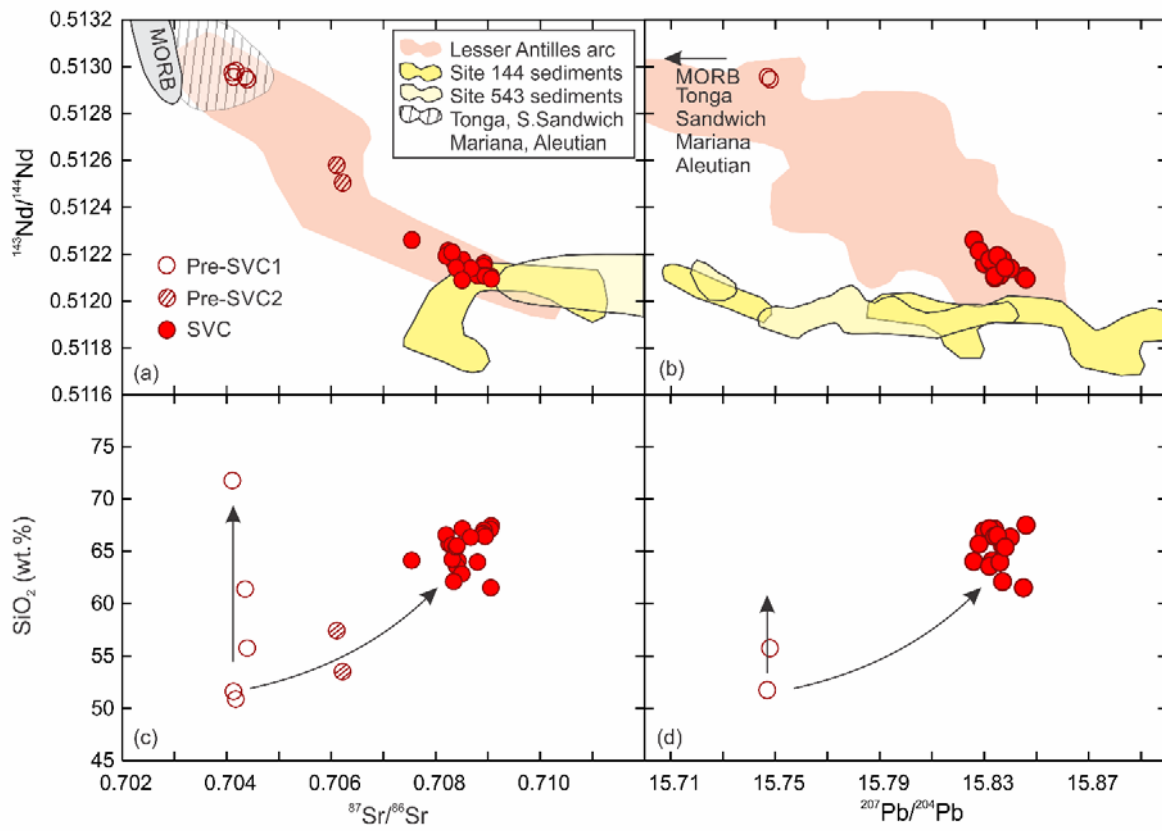


Fig. 3

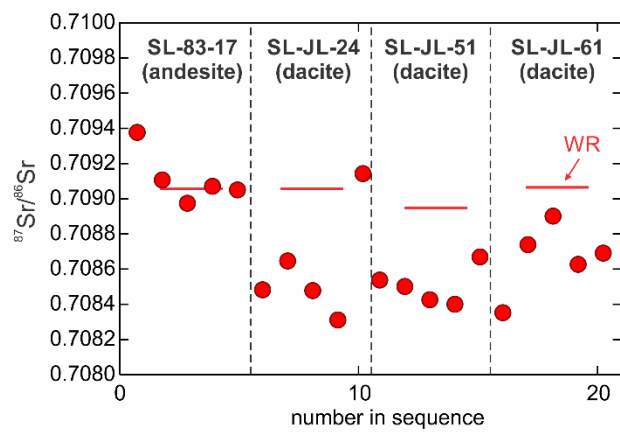


Fig. 4

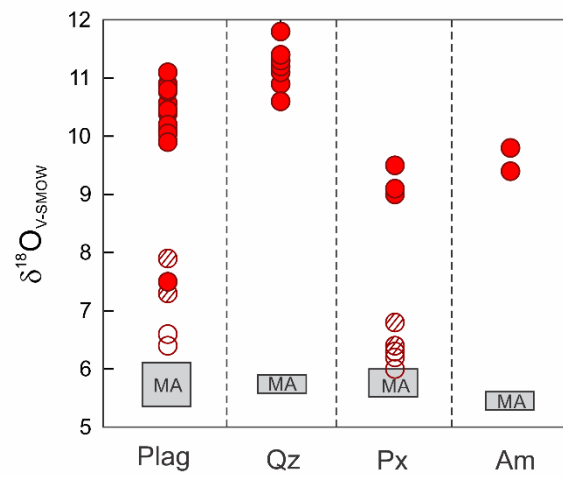


Fig. 5

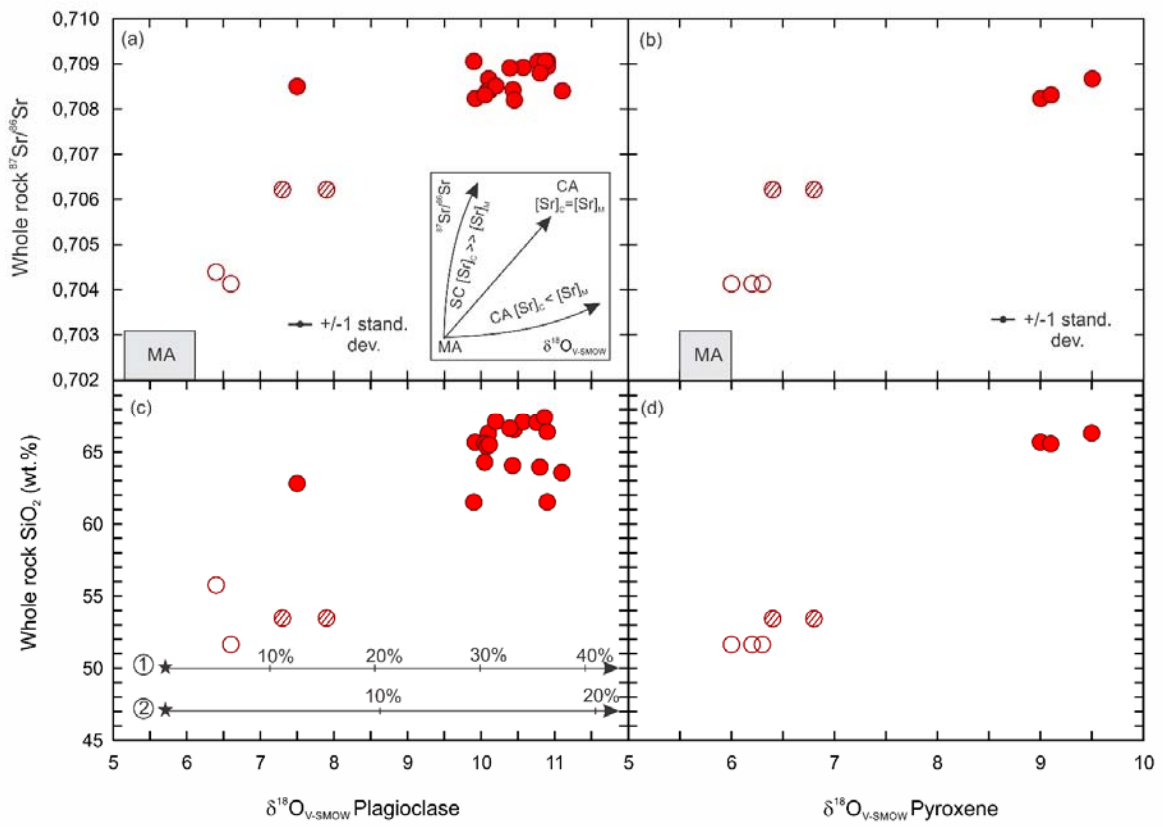


Fig. 6

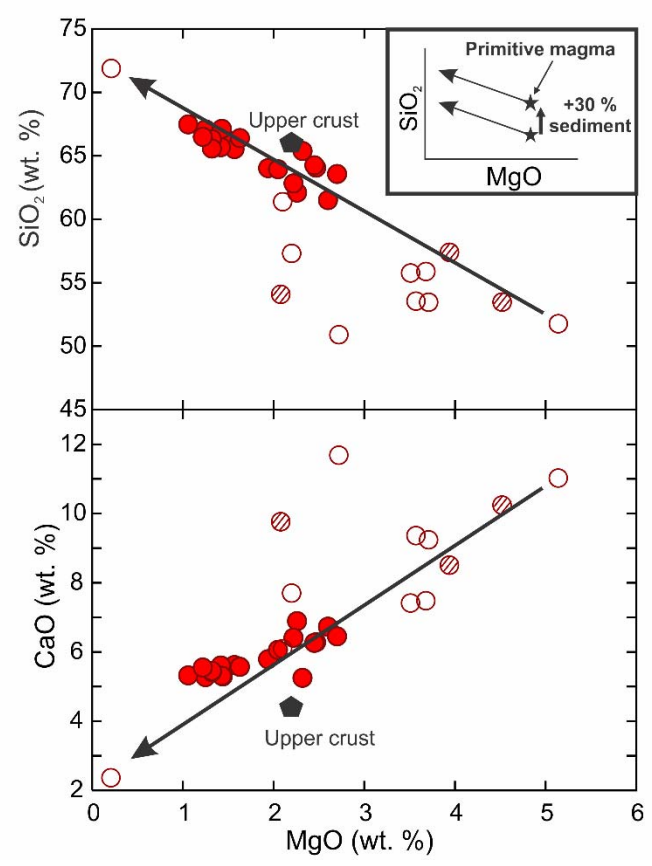


Fig. 7

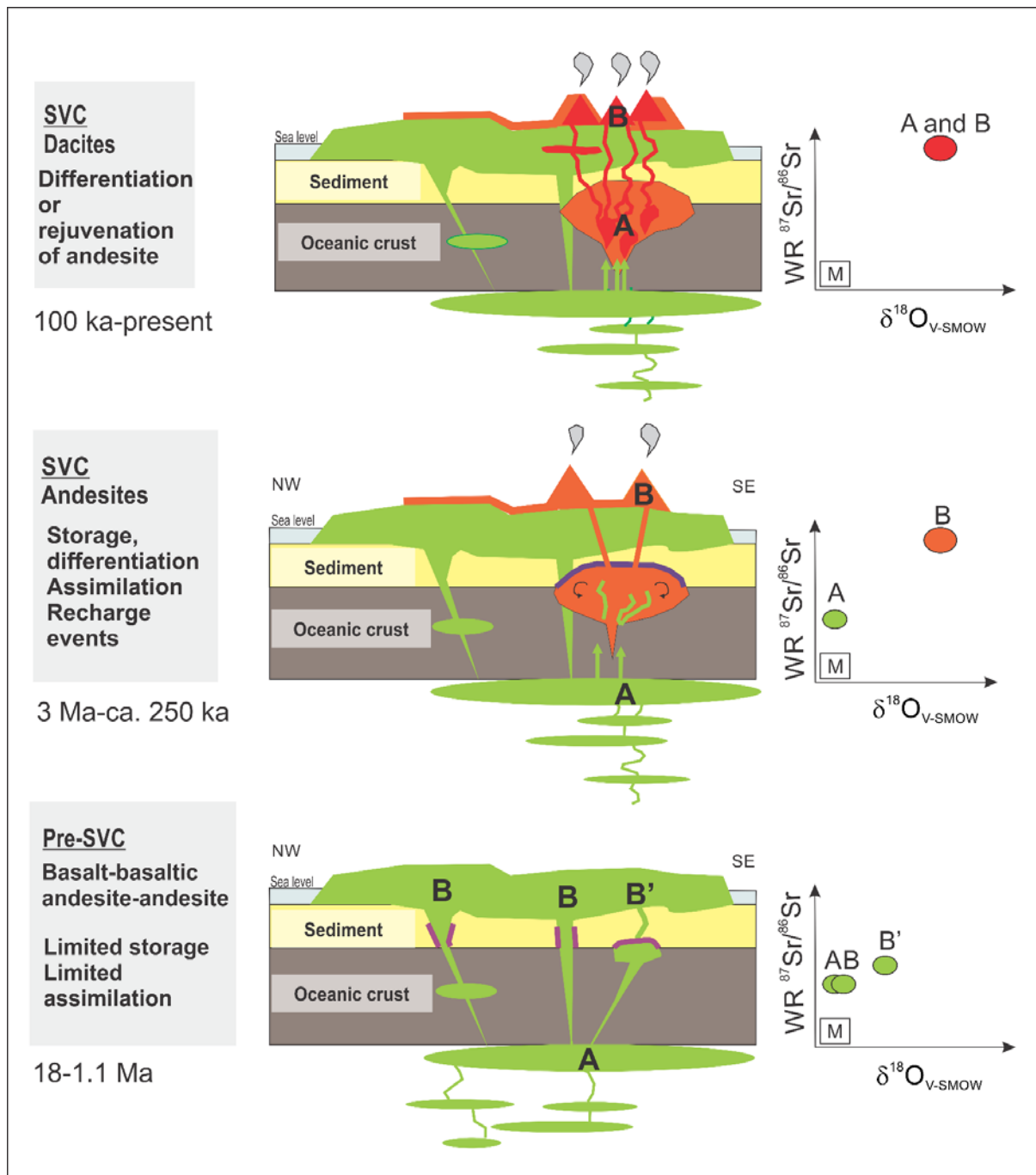


Table 1: St Lucia whole rock Sr-Nd-Pb isotopic compositions and the corresponding SiO₂ and CaO content in wt.%. SiO₂ and CaO concentrations are from Davidson (1987) and Lindsay et al. (2013), and normalised to 100% volatile free.

Durham University							
Sample name	¹⁴³ Nd/ ¹⁴⁴ Nd	⁸⁷ Sr/ ⁸⁶ Sr	²⁰⁶ Pb/ ²⁰⁴ Pb	²⁰⁷ Pb/ ²⁰⁴ Pb	²⁰⁸ Pb/ ²⁰⁴ Pb	SiO ₂	CaO
SL8303	0.512261	0.707542	19.728	15.826	39.438	64	5.79
SL8308	0.512161	0.708925	19.721	15.830	39.457	66.9	5.36
SL8312	0.512147	0.708914	-	-	-	66.7	5.29
SL8315	0.512169	0.708346	19.760	15.837	39.467	62.1	6.89
SL8316	0.512161	0.70843	19.737	15.833	39.466	64.1	6.28
SL8317	0.512106	0.709056	19.797	15.845	39.489	61.5	6.73
SL8319	0.51218	0.708412	19.748	15.837	39.479	65.5	5.62
SL8324	0.512215	0.708237	19.730	15.828	39.446	65.7	5.61
SL8325	0.512946	0.704394	19.291	15.748	38.930	55.8	7.41
SL8344	0.512957	0.704132	19.341	15.747	39.110	51.8	11.02
SL-JL-22	0.512178	0.708402	19.753	15.832	39.471	63.6	6.45
SL-JL-23	0.512111	0.708801	19.779	15.836	39.479	63.9	6.06
SL-JL-24	0.512101	0.709049	19.770	15.834	39.484	67.1	5.27
SL-JL-33	0.512177	0.708511	19.759	15.832	39.473	67.1	5.31
SL-JL-51	0.512108	0.708946	19.766	15.834	39.484	66.4	5.57
SL-JL-57	0.51214	0.708672	19.773	15.840	39.489	66.3	5.42
SL-JL-61	0.512096	0.709063	19.782	15.846	39.528	67.5	5.32
SL-JL-79	0.512187	0.708313	-	-	-	65.6	5.45
SL-JL-83	0.512194	0.708202	19.758	15.835	39.483	66.5	5.55
SL-JL-84	0.512209	0.708313	-	-	-	64.3	6.26
Macquarie University							
Sample name	¹⁴³ Nd/ ¹⁴⁴ Nd	⁸⁷ Sr/ ⁸⁶ Sr	²⁰⁶ Pb/ ²⁰⁴ Pb	²⁰⁷ Pb/ ²⁰⁴ Pb	²⁰⁸ Pb/ ²⁰⁴ Pb	SiO ₂	CaO
SL8326	0.512505	0.706219	-	-	-	53.5	10.24
SL8339	0.51258	0.706106	-	-	-	57.4	8.53
SL8341	0.512958	0.704354	-	-	-	61.4	6.09
SL8342	0.512983	0.704174	-	-	-	50.9	11.68
SL8345	0.512975	0.704109	-	-	-	71.9	2.37
SL-JL-1	0.512143	0.708393	19.757	15.838	39.489	65.4	5.25
SL-JL-2	0.512091	0.708504	-	-	-	62.8	6.41

Table 2: $^{87}\text{Sr}/^{86}\text{Sr}$ of single plagioclase grains separated from four of the most continental-like SVC hand samples. Whole rock SiO_2 (wt. %) and $^{87}\text{Sr}/^{86}\text{Sr}$ are also shown (see Table 1 for references).

Sample name	$^{87}\text{Sr}/^{86}\text{Sr}$	2 SE	Whole rock $^{87}\text{Sr}/^{86}\text{Sr}$	Whole rock SiO_2
SL8317PI1	0.709377	0.000010	0.709056	61.5
SL8317PI2	0.709107	0.000009		
SL8317PI3	0.708974	0.000013		
SL8317PI4	0.709071	0.000009		
SL8317PI5	0.709050	0.000008		
SL-JL-24PI6	0.708482	0.000006	0.709049	67.1
SL-JL-24PI7	0.708646	0.000005		
SL-JL-24PI8	0.708478	0.000010		
SL-JL-24PI9	0.708311	0.000007		
SL-JL-24PI10	0.709143	0.000009		
SL-JL-51PI11	0.708538	0.000007	0.708946	66.4
SL-JL-51PI12	0.708501	0.000010		
SL-JL-51PI13	0.708426	0.000007		
SL-JL-51PI14	0.708400	0.000007		
SL-JL-51PI15	0.708669	0.000005		
SL-JL-61PI16	0.708352	0.000008	0.709063	67.5
SL-JL-61PI17	0.708739	0.000006		
SL-JL-61PI18	0.708901	0.000007		
SL-JL-61PI19	0.708627	0.000007		
SL-JL-61PI20	0.708691	0.000006		

Table 3: $\delta^{18}\text{O}$ of single mineral separates from St Lucia along with the corresponding whole rock SiO_2 (wt.%) and Sr isotopic composition. WR = whole rock. SiO_2 content from Davidson (1987) and Lindsay et al. (2013) and normalised to 100% volatile free.

Sample name	Kind of mineral	Group	$\delta^{18}\text{O}_{\text{V-SMOW}}$ (‰)	WR SiO_2	WR $^{87}\text{Sr}/^{86}\text{Sr}$
8308PI	Plagioclase	SVC	10.6	66.9	0.708925
8312PI	Plagioclase	SVC	10.4	66.7	0.708914
8316PI	Plagioclase	SVC	10.4	64.1	0.70843
8317PI	Plagioclase	SVC	10.9	61.5	0.709056
8317PI	Plagioclase	SVC	9.9	61.5	0.709056
8319PI	Plagioclase	SVC	10.1	65.5	0.708412
8324PI	Plagioclase	SVC	9.9	65.7	0.708237
8325PI	Plagioclase	Pre-SVC1	6.4	55.8	0.704394
8326PI1	Plagioclase	Pre-SVC2	7.3	53.5	0.706219
8326PI2	Plagioclase	Pre-SVC2	7.9	53.5	0.706219
8344PI	Plagioclase	Pre-SVC1	6.6	51.8	0.704132
JL01PI	Plagioclase	SVC	10.1	65.4	0.708393
JL02PI	Plagioclase	SVC	7.5	62.8	0.708504
JL22PI	Plagioclase	SVC	11.1	63.6	0.708402
JL23PI	Plagioclase	SVC	10.8	63.9	0.708801
JL24PI	Plagioclase	SVC	10.8	67.1	0.709049
JL33PI	Plagioclase	SVC	10.2	67.1	0.708511
JL51PI	Plagioclase	SVC	10.9	66.4	0.708946
JL57PI	Plagioclase	SVC	10.1	66.3	0.708672
JL61PI	Plagioclase	SVC	10.9	67.5	0.709063
JL83PI	Plagioclase	SVC	10.5	66.5	0.708202
JL84PI	Plagioclase	SVC	10.0	64.3	0.708313
JL79PI	Plagioclase	SVC	10.0	65.6	0.708313
8303Qz	Quartz	SVC	11.2	64.0	0.707542
JL01Qz	Quartz	SVC	11.3	65.4	0.708393
JL02Qz	Quartz	SVC	11.4	62.8	0.708504
JL22Qz	Quartz	SVC	11.3	63.6	0.708402
JL23Qz	Quartz	SVC	10.9	63.9	0.708801
JL24Qz	Quartz	SVC	11.4	67.1	0.709049
JL33Qz	Quartz	SVC	11.1	67.1	0.708511
JL51Qz	Quartz	SVC	11.3	66.4	0.708946
JL57Qz	Quartz	SVC	10.6	66.3	0.708672
JL61Qz	Quartz	SVC	11.8	67.5	0.709063
8324Opx	Orthopyroxene	SVC	9	65.7	0.708237
8326Py1	Clinopyroxene	Pre-SVC2	6.8	53.5	0.706219
8326Py2	Clinopyroxene	Pre-SVC2	6.4	53.5	0.706219
8344Py1	Clinopyroxene	Pre-SVC1	6.0	51.8	0.704132
8344Py2	Clinopyroxene	Pre-SVC1	6.2	51.8	0.704132
8344Py3	Clinopyroxene	Pre-SVC1	6.3	51.8	0.704132
JL57Opx	Orthopyroxene	SVC	9.5	66.3	0.708672
JL79Opx	Orthopyroxene	SVC	9.1	65.6	0.708313
8308Am	Amphibole	SVC	9.8	66.9	0.708925
JL33Am	Amphibole	SVC	9.4	67.1	0.708511